Diffraction of ultracold fermions by quantized light fields: Standing versus traveling waves

D. Meiser, C. P. Search,* and P. Meystre

Optical Sciences Center, The University of Arizona, Tucson, Arizona 85721, USA
(Received 21 February 2004; published 7 January 2005)

We study the diffraction of quantum-degenerate fermionic atoms off of quantized light fields in an optical cavity. We compare the case of a linear cavity with standing-wave modes to that of a ring cavity with two counterpropagating traveling wave modes. It is found that the dynamics of the atoms strongly depends on the quantization procedure for the cavity field. For standing waves, no correlations develop between the cavity field and the atoms. Consequently, standing-wave Fock states yield the same results as a classical standing wave field while coherent states give rise to a collapse and revivals in the scattering of the atoms. In contrast, for traveling waves the scattering results in quantum entanglement of the radiation field and the atoms. This leads to a collapse and revival of the scattering probability even for Fock states. The Pauli exclusion principle manifests itself as an additional dephasing of the scattering probability.

PACS number(s): 42.50.Vk, 03.75.Ss, 42.50.Pq

I. INTRODUCTION

The past few decades have witnessed considerable progress in the cooling of atomic vapors to extremely low temperatures, culminating in the achievement of Bose-Einstein condensation in dilute alkali-metal gases [1–3]. More recently, quantum-degenerate Fermi gases with temperatures as low as 0.01 T_F, where T_F is the Fermi temperature, have been achieved by several groups [4–6]. Throughout these developments the interaction of light with atoms has been central to the cooling, trapping, and imaging of atoms, as well as in the coherent manipulation of their center-of-mass motion. For example, the Bragg scattering of atomic matter waves by off-resonant optical fields can be used to create linear atom optical elements for use in atom interferometers [7], and the interaction of atomic condensates with light has led to the realization of matter-wave superradiance [8] and of matter-wave parametric amplifiers [9–11]. In another application, the ability of optical fields to create custom trapping potentials has permitted the study of condensed matter problems such as, e.g., the Mott-insulator transition [12–14]. Although all experiments to date have involved classical optical fields, there is considerable interest in carrying out future work in high-Q optical cavities, where the quantum nature of the electromagnetic field becomes important. Theoretical work along these lines has so far been restricted to the case of bosonic atoms (see, e.g., Ref. [15]), while the diffraction of fermions by an optical field was discussed in Ref. [16], but in an analysis restricted to the case of classical fields. In this paper we extend this work to discuss the diffraction of quantum-degenerate fermionic matter-wave fields by quantized light fields.

We consider a zero-temperature beam of fermionic two-level atoms traversing an optical cavity supporting an off-resonant standing-wave light field of momentum q. The atoms undergo virtual transitions to their excited electronic state, resulting in a center-of-mass momentum recoil of $2q$. Alternatively, one can view this process as diffraction the atoms off the intensity grating formed by the cavity field.

The normal modes in terms of which the electromagnetic field is quantized are determined by the boundary conditions of the cavity. A linear cavity with perfectly reflecting mirrors is described in terms of standing-wave mode functions. In a ring cavity, in contrast, the light field has to satisfy periodic boundary conditions and this results in running-wave mode functions. Two counterpropagating traveling-wave modes of equal frequency can be superposed to yield a stationary standing-wave field.

Under most circumstances it is a question of mathematical convenience which mode functions are used for the description of the field. Physically, however, the two cases are not the same and for fields containing only a few photons, the two quantization procedures yield different results. In particular, the difference in atomic scattering produced in these two situations has been discussed for single atoms diffracted by a coherent light field [17]. Diffraction was shown to depend critically on the quantization procedure, a difference that can be understood in terms of which-way information for the scattering process. For standing-wave modes, the state of the light field contains no information about the momentum transfer to the atom. More specifically, the number of photons is a constant of motion and as a result the equations of motion for the atomic center of mass decouple from that of the light field. In the case of two counterpropagating traveling-wave modes however, the number of photons in each mode does change and the change in the number of quanta is a direct measure of the momentum transfer to the atoms. In this paper we extend those results to compare the diffraction of a quantum-degenerate Fermi gas by these fields, in both the Raman-Nath and Bragg regimes.

In the Raman-Nath regime, which is characteristic of situations where the kinetic energy of the atoms can be neglected, the individual atomic dynamics for a standing-wave light field are formally identical to the case of a classical light field [18]. The atoms scatter into successive diffraction orders separated by twice the photon momentum q, up to the point where energy-momentum conservation becomes important and the Raman-Nath approximation ceases to hold.

---

*Present address: Department of Physics and Engineering Physics, Stevens Institute of Technology, Castle Point on Hudson, Hoboken, NJ 07030, USA.

The formal equivalence of the scattering off a standing-wave field to the scattering off a classical light field is due to the fact that the equations of motion for the atoms effectively decouple both from each other and from the light field. This must be contrasted to the case of running waves, where the number operators for the two modes are not constants of motion. This leads to an infinite hierarchy of coupled equations for the atomic and optical field operators, with higher-order correlation functions playing a crucial role in the dynamics of first-order atomic correlation functions. To proceed analytically it is then necessary to introduce some approximate truncation scheme, a procedure that we discuss in detail and compare with exact numerical results for small atom numbers.

In the Bragg regime, energy-momentum conservation reduces the single-atom diffraction problem to a two-mode situation, the atoms undergoing Bragg oscillations between their initial momentum states p_i and final momentum state $p_f = p_i + 2q$. The character of these oscillations is the result of three separate and independent effects that correspond to whether one uses standing-wave or traveling-wave modes, whether the cavity field is in a Fock state or in a coherent state, and the momentum spread of the incident atomic beam.

This paper is organized as follows. After formulating our model in Sec. II we discuss the case of traveling-wave light quantization in Sec. III. We develop approximate equations for first- and second-order correlation functions appropriate for the Raman-Nath regime, and a Bloch vector picture useful to discuss Bragg diffraction. That picture yields a semiclassical model that provides some intuitive understanding of the atomic dynamics. The case of standing-wave quantization is discussed in Sec. IV, and Sec. V gives a summary and conclusion.

II. MODEL

We consider an ultracold beam of identical two-level fermionic atoms propagating across a high-Q optical cavity; see Fig. 1. Their initial momentum distribution is a Fermi sea at $T=0$, but shifted in momentum space by the mean momentum **p** and with Fermi momentum k_F assumed to be much less than q, the photon momentum. This is a realistic approximation, since for a degenerate Fermi gas of density $n \approx 10^{17}$ m^{-3} the Fermi momentum is $k_F \approx 10^6$ m^{-1} while for a photon of wavelength $\lambda = 500$ nm one has a momentum of $q \approx 10^7$ m^{-1}. Consistently with typical experimental conditions we also assume that the number of atoms N_a, given in three dimensions by

$$N_a = \frac{Vk_F^3}{6\pi^2},$$ (1)

where V is the quantization volume, is much less than the number of photons N_p. Note that as is typically the case with fermions, the memory requirements of a numerical calculation scale as 2^{N_a}, limiting the number of particles that can typically be handled in practice to less than 20. In addition, the quantized nature of the light field can significantly further reduce this number.
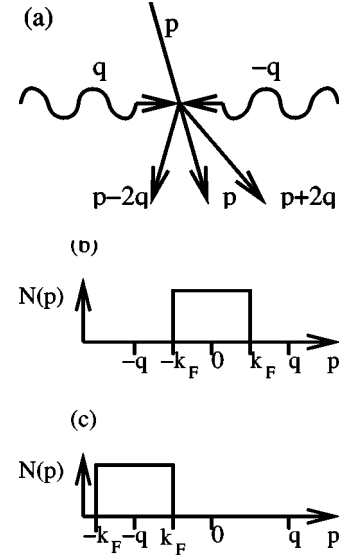

FIG. 1. (a) Schematic of a scattering of an atom of initial momentum p via two-photon transitions with photons of momenta q and $-q$. Initial momentum distribution $N(p)$ of the atoms for scattering in (b) the Raman-Nath regime and (c) the Bragg regime.

In the following we neglect atomic collisions—a good approximation well below the Fermi temperature, since the s-wave scattering length is zero for identical fermions—as well as decay of the optical field in the cavity. We also assume that the optical frequency ω is sufficiently detuned from the atomic transition frequency ω_0 that the upper electronic level can be adiabatically eliminated. Finally, we consider a situation where that atomic momentum $mv_\perp$ transverse to the cavity field is large enough to be treated classically. Time t can then be parametrized in terms of the transverse distance x by $t = x/v_\perp$.

III. RUNNING WAVES

For running-wave quantization, the Hamiltonian describing our system is ($\hbar = 1$)

$$H_r = \sum_k E_k c_k^\dagger c_k + \omega(a_q^\dagger a_q + a_{-q}^\dagger a_{-q} + 1)$$

$$+ (g a_q^\dagger a_{-q} \sum_k c_{k-q}^\dagger c_{k+q} + \text{H.c.}),$$ (2)

where c_k and $c_k^\dagger$ are the annihilation and creation operators for a fermionic atom of momentum k, a_q and $a_q^\dagger$ are the annihilation and creation operators for a photon of momentum q, $E_k = k^2/2M$ is the kinetic energy of an atom of momentum k, $g = \Omega_R^2/\Delta$ is the coupling energy of the atoms and the light field, Ω_R is the vacuum Rabi frequency, and $\Delta = \omega - \omega_0$ is the atom-light detuning.

The initial state of the atoms-field system is

$$|\psi(0)\rangle_{\text{rw}} = |\phi_q\rangle |\phi_{-q}\rangle \prod_{|k| < k_F} c_k^\dagger |0\rangle,$$ (3)

where the field states $|\phi_{\pm q}\rangle$ are taken to be either Fock states $|N_{\pm q}\rangle$ or coherent states $|\alpha_{\pm q}\rangle$.
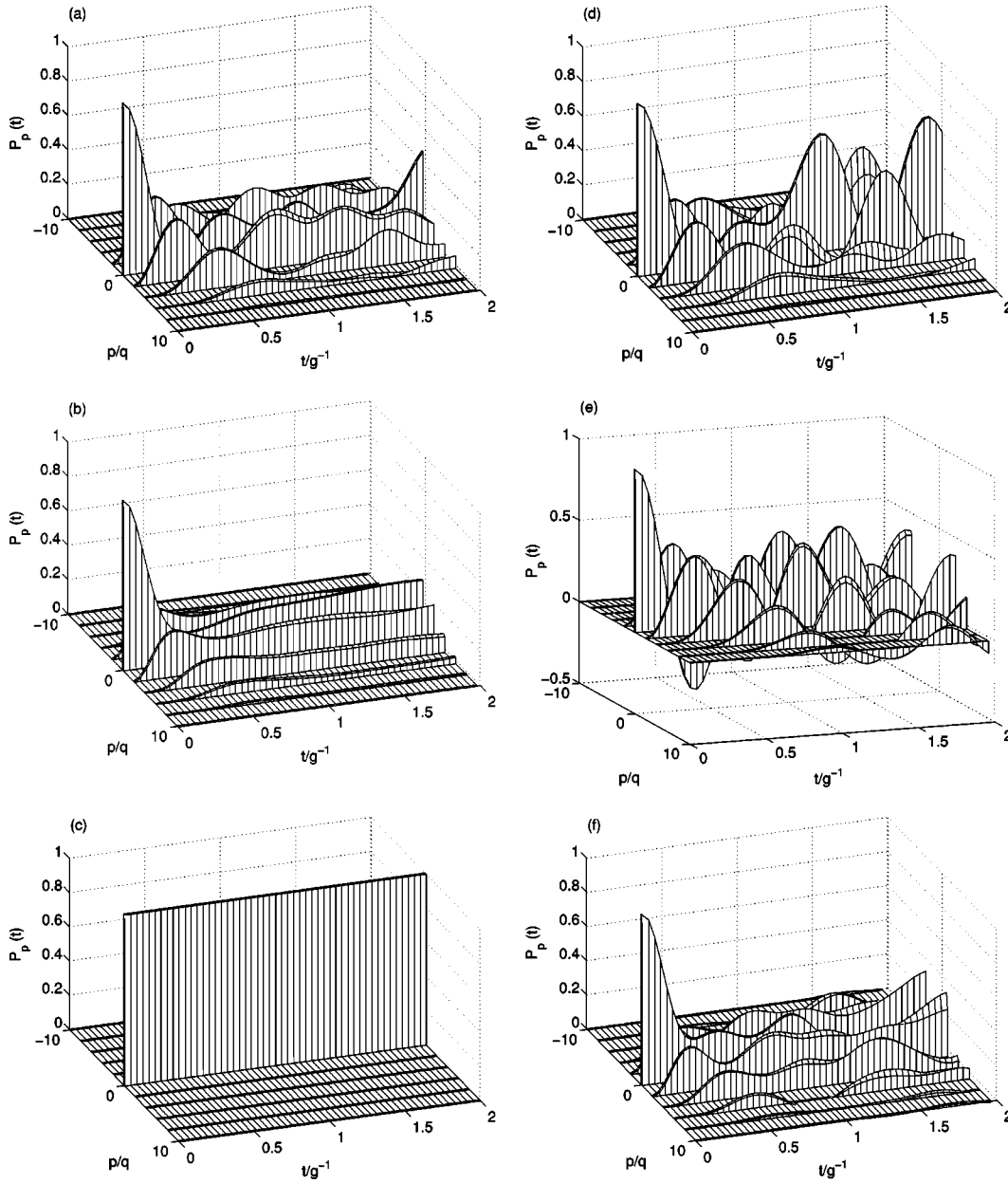
FIG. 2. Scattering probability $P_p(t)$ for two atoms scattering off a running-wave light field in the Raman-Nath regime. (a),(c),(e) are for a Fock state of the light field and (b),(d),(f) for a coherent state. (a),(b) Exact solution; (c),(d) results of first-order equations; (e),(f) results for the second-order equations. $E_{2q}=g$, $k_F=0.1$, time in units of g^{-1}, momentum in units of q.

A. Raman-Nath regime

The Raman-Nath regime is characteristic of situations where the kinetic energy of the atoms plays a negligible role in comparison with the interaction energy, i.e., $E_{2q} \ll g\sqrt{N_q N_{-q}}$, where the recoil energy $E_{2q}=2q^2/M$ is a measure for the typical kinetic energies involved. In practice, this amounts to assuming that the atoms have an infinite mass, and as such, neglects the effects of the quadratic dispersion relation of the atoms.

The most straightforward way to solve this problem proceeds by integrating the Schrödinger equation corresponding to Hamiltonian (2) for the initial conditions (3), from which we can obtain the probability

$$P_p(t) = \langle \psi(t) | c_p^\dagger c_p | \psi(t) \rangle \qquad (4)$$

for an atom being scattered to a state of momentum p. However, the dimension D of the Hilbert space grows exponentially as $D_{\text{Raman-Nath}}=(2n_d+1)^{N_a}(N_p+1)$ where n_d is the number of diffraction orders considered. Hence, a direct integration of the Schrödinger equation is possible only for rather small atom and photon numbers.

Figure 2(a) shows the result of an exact solution of the Schrödinger equation for $N_a=2$ atoms and the light field initially in a Fock state with three photons per mode. In this example, the recoil energy is $E_{2q}=g$ and the initial momentum of the atoms is $p_i=\pm 0.1q$. Such a high recoil energy was

chosen to limit the number of diffraction orders that are significantly populated before energy-momentum conservation inhibits further diffraction, i.e., before exiting the Raman-Nath regime.

The resulting dynamics resembles qualitatively the single-atom case; see, e.g., [18]. For short times the probability of finding an atom in the mth-order mode is well described by $\sim J_m^2(2gt)$ where J_m is the mth Bessel function. For longer interaction times, higher scattering orders are suppressed due to energy-momentum conservation, as expected. We note that since the difference in kinetic energies of the two atoms is small compared to all other relevant energies, we do not observe any effect of "inhomogeneous broadening."

For comparison, the results for initial coherent states with mean photon numbers $\bar{N}_q = \bar{N}_{-q} = 3$ are shown in Fig. 2(b) for the same atomic parameters. We now observe a decay of the oscillations of the scattering probabilities after a time $t \sim (2\pi/g)(\bar{N}_q\bar{N}_{-q})^{-1/2}$, which corresponds to a complete dephasing of the contributions of the different photon numbers to the diffraction pattern.

Experimentally, the most directly accessible quantity describing the scattering dynamics of the atoms is the first-order correlation function $\langle c_{k_1}^\dagger c_{k_2} \rangle$. From the Hamiltonian (2) we find readily

$$i\frac{d}{dt}\langle c_{k_1}^\dagger c_{k_2} \rangle = (E_{k_2} - E_{k_1})\langle c_{k_1}^\dagger c_{k_2} \rangle + g\langle a_{-q}^\dagger a_q (c_{k_1}^\dagger c_{k_2-2q} \\ - c_{k_1+2q}^\dagger c_{k_2})\rangle + g\langle a_q^\dagger a_{-q}(c_{k_1}^\dagger c_{k_2+2q} - c_{k_1-2q}^\dagger c_{k_2})\rangle,$$
(5)

$$i\frac{d}{dt}\langle a_{q_1}^\dagger a_{q_2} \rangle = g\sum_k \langle \delta_{q_2,q} a_{q_1}^\dagger a_{-q} c_{k-q}^\dagger c_{k+q} + \delta_{q_2,-q} a_{q_1}^\dagger a_q c_{k+q}^\dagger c_{k-q} \\ + \delta_{q_1,-q} a_q^\dagger a_{q_2} c_{k-q}^\dagger c_{k+q} + \delta_{q_1,q} a_{-q}^\dagger a_{q_2} c_{k+q}^\dagger c_{k-q}\rangle,$$
(6)

where the δ's are Kronecker delta functions.

Because the response of the atoms to the light field is nonlinear, the first-order correlations are coupled to second-order correlations, which in turn will be coupled to third-order correlations, and so on. Thus, we end up with an infinite hierarchy of equations of motions for the correlation functions of all orders. This hierarchy of equations is reminiscent of the so-called Bogoliubov-Born-Green-Kirkwood-Yvon (BBGKY) hierarchy encountered in the theory of interacting gases; see, e.g., Ref. [19], p. 65. In order to get a closed set of c-number equations we need to invoke a factorization scheme that truncates this hierarchy. The resulting set of ordinary differential equations can then be solved by standard numerical techniques and the number of equations grows only polynomially with the number of atoms.

The simplest and most naive factorization scheme consists in simply factorizing second-order correlation functions of the type $\langle a_{q_1}^\dagger a_{q_2} c_{k_1}^\dagger c_{k_2} \rangle$ that appear on the right-hand side of Eqs. (5) and (6) into products of first-order correlation functions, for instance, $\langle a_{q_1}^\dagger a_{q_2} c_{k_1}^\dagger c_{k_2} \rangle \approx \langle a_{q_1}^\dagger a_{q_2}\rangle\langle c_{k_1}^\dagger c_{k_2} \rangle$. In doing so we neglect correlations that may build up between the

atoms and the light field as well as higher-order atom-atom and field-field correlations. The result of the numerical integration of these equations of motion is shown in Figs. 2(c) and 2(d) for the cases of a Fock state and a coherent state of the field, respectively.

An obvious weakness of the simple truncation scheme is that it predicts the absence of scattering for the case of Fock states, in stark contrast to the exact solution. This follows from the absence of initial coherence in either the light field or the atoms, leading to the scattering term in Eq. (5) being identically zero. Stated differently, the reason for the absence of diffraction is that the phase of a Fock state is completely undetermined, hence there is no established relative phase between the two counterpropagating fields, and no light intensity grating. Since in this factorization scheme the atom is effectively assumed to probe only first-order moments of the light field, that is, its intensity pattern, diffraction is absent at this level of approximation.

The situation is different for a coherent state light field. In this case, there is a well-established phase relationship between the two modes. This results in an intensity grating from which the atoms can be diffracted. As time goes on, this results in the generation of atomic coherence, $\langle c_{k_1}^\dagger c_{k_2} \rangle \neq 0$, and the resulting density grating formed by the atoms acts back on the light field. In some loose sense, the lowest-order factorization scheme consists in treating the system classically since it neglects all quantum fluctuations in the atomic and optical fields. It is not surprising that this approach should fail for a very nonclassical field state such as a Fock state, and be much better for a quasiclassical field. Note, however, that while for short enough times the scattering closely resembles the exact results, this is no longer the case for long times, a consequence of the buildup of quantum correlations between the optical and matter-wave fields.

We note that for our specific initial conditions, the fully factorized equations for the light field can be trivially integrated, showing that the first-order moments of the light field are constants of motion. Inserting these constants in the atomic equations of motion shows that at this level, the scattering becomes formally equivalent to the scattering of atoms by a classical standing-wave light field with intensity $g\langle a_q^\dagger a_{-q}\rangle$. This is further discussed in the following section.

The equations of motion (5) and (6), suggest that an improved factorization scheme would retain the lowest-order correlations between light field and atoms. In order to do so, we supplement the equations of motion for $\langle c_{k_1}^\dagger c_{k_2} \rangle$ and $\langle a_{q_1}^\dagger a_{q_2} \rangle$ by equations of motion for the cross correlations $\langle a_{q_1}^\dagger a_{q_2} c_{k_1}^\dagger c_{k_2} \rangle$ and the second-order correlations of the light field and the atoms. This should remedy the major flaw of the first-order calculation, namely, its inability to predict atomic scattering for a light field in a Fock state.

The equations for the lowest-order atom-field correlation functions involve third-order correlations of the form $\langle a_{q_1}^\dagger a_{q_2} a_{q_3}^\dagger a_{q_4} c_{k_1}^\dagger c_{k_2} \rangle$ and $\langle a_{q_1}^\dagger a_{q_2} c_{k_1}^\dagger c_{k_2} c_{k_3}^\dagger c_{k_4} \rangle$. We truncate the resulting hierarchy of equations of motion by introducing the factorization scheme

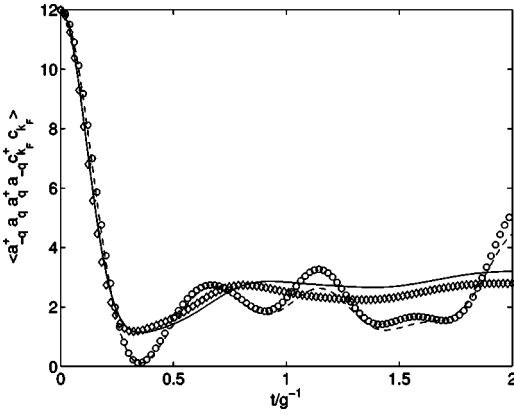FIG. 3. Expectation value of $a^\dagger_{-q}a_q a^\dagger_q a_{-q}c^\dagger_{k_F}c_{k_F}$ from the numerical solution of the Schrödinger equation for a Fock state and for a coherent state; same parameters as in Fig. 2. ○ and ◇, exact (unfactorized) value for Fock state and coherent state respectively; broken line (−−) and solid line (—), corresponding values for the Fock state and coherent state as obtained with the factorization scheme (7).

$$\langle a^\dagger_{q_1}a_{q_2}a^\dagger_{q_3}a_{q_4}c^\dagger_{k_1}c_{k_2}\rangle \simeq \langle a^\dagger_{q_1}a_{q_2}\rangle\langle a^\dagger_{q_3}a_{q_4}c^\dagger_{k_1}c_{k_2}\rangle + \langle a^\dagger_{q_1}a_{q_2}a^\dagger_{q_3}a_{q_4}\rangle$$
$$\times\langle c^\dagger_{k_1}c_{k_2}\rangle + \langle a^\dagger_{q_1}a_{q_2}c^\dagger_{k_1}c_{k_2}\rangle\langle a^\dagger_{q_3}a_{q_4}\rangle$$
$$- 2\langle a^\dagger_{q_1}a_{q_2}\rangle\langle a^\dagger_{q_3}a_{q_4}\rangle\langle c^\dagger_{k_1}c_{k_2}\rangle \qquad (7)$$

and similarly for $\langle a^\dagger_{q_1}a_{q_2}c^\dagger_{k_1}c_{k_2}c^\dagger_{k_3}c_{k_4}\rangle$ with a_q's replaced by c_k's, and vice versa [20]. The last term of this equation accounts for the case where all first-order correlation functions are uncorrelated. Background information on the motivation for this kind of factorization scheme can be found in Chapter 4 of [21].

We estimate the accuracy of the factorization scheme by calculating $\langle a^\dagger_{q_1}a_{q_2}a^\dagger_{q_3}a_{q_4}c^\dagger_{k_1}c_{k_2}\rangle$ and $\langle a^\dagger_{q_1}a_{q_2}c^\dagger_{k_1}c_{k_2}c^\dagger_{k_3}c_{k_4}\rangle$ as well as their respective factorized values Eq. (7) using the exact solution of the Schrödinger equation. As an example Fig. 3 shows the results for $\langle a^\dagger_{-q}a_q a^\dagger_q a_{-q}c^\dagger_{k_F}c_{k_F}\rangle$ and Fig. 4 shows the results for $\langle a^\dagger_q a_q c^\dagger_{k_F}c_{k_F}c^\dagger_{k_F}c_{k_F}\rangle$ for the parameters of Fig. 2. This shows that the factorization scheme reproduces at least qualitatively the main features of the third-order correlation functions for both coherent states and Fock states.

Despite its partial success, this factorization scheme suffers from two major flaws. First, the small deviations of the factorized values from the exact values accumulate in time, leading to increasing discrepancies between the approximate and exact results. Even worse, this scheme violates important relations that the exact operators have to obey. For example, $a^\dagger_q a_q c^\dagger_{k_F}c_{k_F}c^\dagger_{k_F}c_{k_F}$ is a positive self-adjoint operator, with positive and real expectation values, but the factorized approximation can take on negative values. These flaws eventually result in the nonphysical behavior illustrated in Figs. 2(e) and 2(f), where the probabilities $\langle c^\dagger_k c_k\rangle$ take on negative values. We have not found a factorization scheme that avoids nonphysical behavior of that kind for all times, and conjecture that the factorization of higher-order moments into
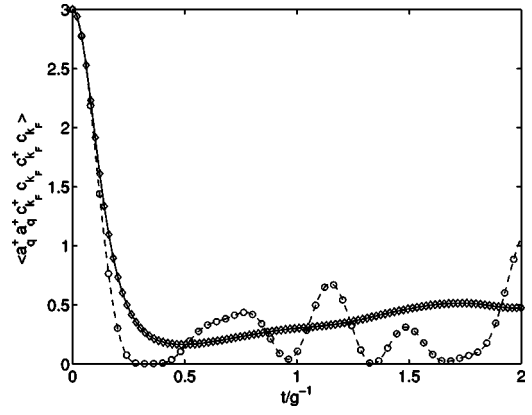

FIG. 4. Expectation value of $a^\dagger_q a_q c^\dagger_{k_F}c_{k_F}c^\dagger_{k_F}c_{k_F}$ from the numerical solution of the Schrödinger equation for a Fock state and for a coherent state of the light field; same parameters as in Fig. 2. ○ and ◇, exact unfactorized value for Fock state and coherent state, respectively; broken line (−−) and solid line (—), results from the factorization scheme (7) for the same two cases.

lower-order moments necessarily leads to such inconsistencies.

The results of the factorization scheme (7) are shown in Fig. 2(e) for a Fock state and in Fig. 2(f) for a coherent state of the light field. While a Fock state now leads to atomic diffraction, as should be the case, it is characterized by nonphysical negative probabilities already for short times. This is clear evidence that higher-order correlations play an essential role. This is in contrast with the situation for a coherent state, where we achieve good agreement with the exact results for times up to $\sim(2\pi/g)(\bar{N}_q\bar{N}_{-q})^{-1/2}$, indicating that the first- and second-order correlations are the most important.

A quantitative measure of the degree of entanglement between the atoms and the light field is given by the second-order cross correlation

$$\chi(t) = \sum_k (\langle a^\dagger_q a_{-q}c^\dagger_{k-q}c_{k+q}\rangle - \langle a^\dagger_q a_{-q}\rangle\langle c^\dagger_{k-q}c_{k+q}\rangle), \qquad (8)$$

which is equal to zero in the absence of entanglement. Figure 5 shows $\chi(t)$ for both a Fock state and a coherent state light field, for the parameters of Fig. 2. Because the light field and atoms are initially uncorrelated we have $\chi(t=0)=0$ but cross correlations then build up to become of the order of $(\bar{N}_q\bar{N}_{-q})^{1/2}N_a$. The figure also shows the result of the factorization ansatz (7), showing the good agreement with the exact result for short enough times.

B. Bragg regime

In the Bragg regime, energy-momentum conservation restricts the scattering of the atoms to two diffraction orders, an initial mode of transverse momentum $p_i \approx -q$ and a final mode of momentum $p_f = p_i + 2q \approx q$. Classically, the atoms are known to undergo Pendellösung oscillations between these two modes. As such, the atoms can be thought of as two-state systems that are conveniently described in terms of pseudospin operators
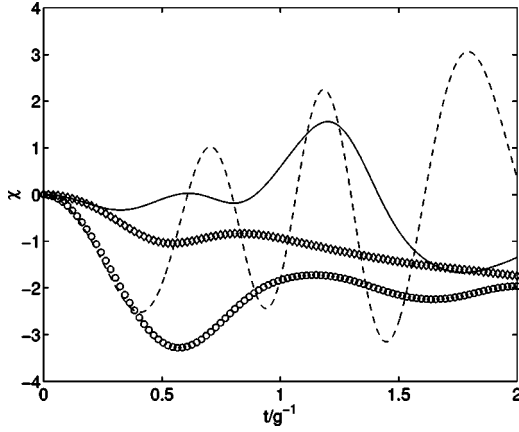
FIG. 5. Cross correlation $\chi(t)$ between light field and atoms in the Raman-Nath regime as obtained from the exact solution of the Schrödinger equation for a Fock state ($\bigcirc$) and a coherent state ($\diamond$) of the light field. Also shown are the values obtained from the factorization scheme (7), (−−) for a Fock state light field and (—) for a coherent state. Same parameters as in Fig. 2.

$$S_k^z = \frac{1}{2}(c_{k+q}^\dagger c_{k+q} - c_{k-q}^\dagger c_{k-q}),$$

$$S_k^+ = (S_k^-)^\dagger = c_{k+q}^\dagger c_{k-q}. \tag{9}$$

Introducing further the Schwinger representation of the light field by means of

$$J^z = \frac{1}{2}(a_q^\dagger a_q - a_{-q}^\dagger a_{-q}),$$

$$J^+ = (J^-)^\dagger = a_q^\dagger a_{-q}, \tag{10}$$

the Hamiltonian of the atoms-field system simplifies to

$$H = \sum_{k \in [-k_F, k_F]} (\delta\omega_k S_k^z + gJ^+ S_k^- + gJ^- S_k^+). \tag{11}$$

In this representation, the eigenvalues m of J^z correspond to the photon number difference $m = (1/2)(N_q - N_{-q})$ between the two counterpropagating modes and the eigenvalues $j(j+1)$ of $J^2 = J^{z2} + 1/2(J^+J^- + J^-J^+)$ correspond to the total number of photons, $j = 1/2(N_q + N_{-q})$. Finally, $\delta\omega_k = E_{k+q} - E_{k-q} = 2kq/M$ is the frequency mismatch between the two momentum states accessible to the atom with initial momentum $k - q$.

When compared to the Raman-Nath case, the dimension of the Hilbert space is now reduced to $D_{\text{Bragg}} = (N_p + 1)2^{N_a}$, which allows us to consider larger numbers of atoms and photons. The initial state of the atoms is now a zero-temperature Fermi sea shifted by $-q$ in momentum, and we evaluate the total number of atoms diffracted to states of momentum near $+q$,

$$N_{sc}(t) = \sum_{k \in [-k_F, k_F]} P_{k+q}(t) \equiv \sum_{p_f} P_{p_f}, \tag{12}$$

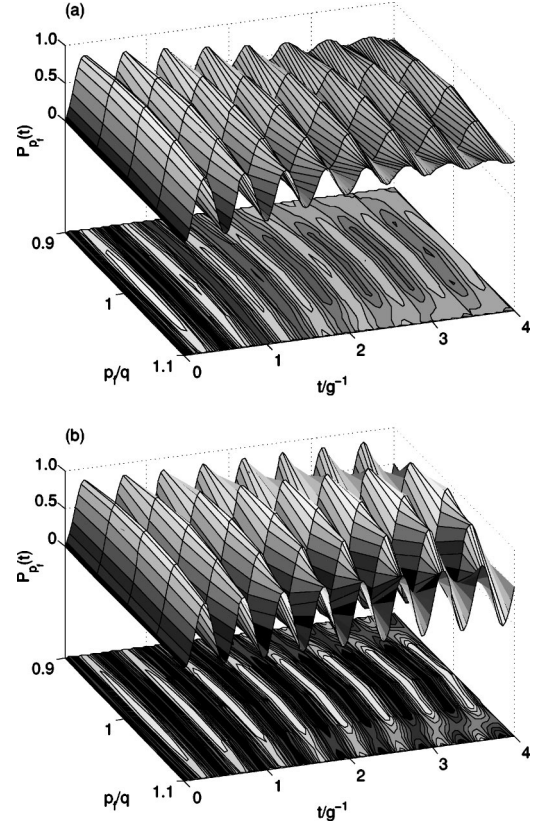for a light field initially in a Fock state and in a coherent state.

FIG. 6. Scattering probability $P_{p_f}(t)$ for five fermions scattering off a running-wave light field (a) and a standing-wave light field (b) in the Bragg regime. The light field is in a Fock state with $N_q = N_{-q} = 6$ and $N = 12$ photons, respectively, $E_{2q} = 50g$, and $k_F = 0.1q$. Time in units of g^{-1} and momentum in units of q.

1. Fock state

Figure 6(a) shows the probability $P_{p_f}(t)$ that an atom has a final momentum p_f in the vicinity of $+q$. In this example, which is for five atoms, the counterpropagating field modes are initially in a Fock state with $N_q = N_{-q} = 6$ photons, the recoil energy is $E_{2q} = 50g$, and the Fermi momentum is $k_F = 0.1q$. Figure 7(a) shows $N_{sc}(t)$ for the same parameters.

For short times the atoms undergo Pendellösung oscillations between initial and final momentum states, with an amplitude that decreases as the atomic momentum is further detuned from the Bragg resonance condition. For longer times the oscillations of the individual atoms dephase, as expected from their different kinetic energies. However, the dephasing is not as strong as would be the case for a system of independent particles, such as in the standing-wave case discussed later on, a clear manifestation of the collective nature of the system.

In addition, the individual atomic oscillations undergo a decay that is intrinsically linked to the quantum correlations that build up between the light field and the atoms and is present even if we neglect dephasing (i.e., $k_F = 0$), as shown in Fig. 7(b). For zero dephasing, the amplitude of the oscillations eventually revives to its initial value. (The fact that the collapse of the oscillations and their subsequent revival resemble a beat phenomenon in the figure is an artifact from
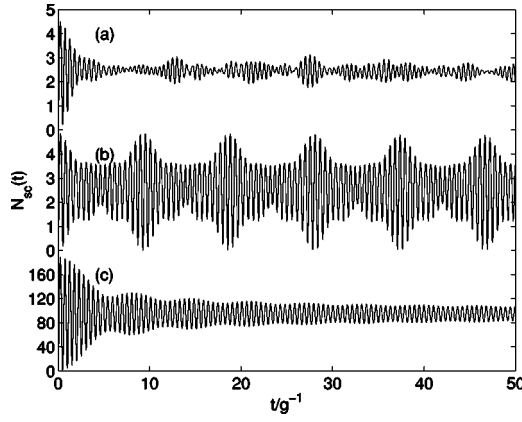
FIG. 7. Mean number of scattered atoms, $N_{sc}=\Sigma P_{pf}$, for Fock states of the light field and for different recoil energies. (a) Running-wave light field with $N_q=N_{-q}=6$ photons in each of the two modes with recoil energy $E_{2q}=50g$. (b) Same light field as in (a) but without dephasing for the atoms, $E_{2q}=0$. (c) Standing-wave light field with $N=6$ photons with recoil energy $E_{2q}=50g$ for 200 atoms. Time in units of g^{-1}.

the comparatively small number of atoms and photons.) Combined with the inhomogeneous dephasing due to the width of the Fermi sea, this decay results in the total oscillation amplitude $N_{sc}(t)$ shown in Fig. 7(a).

We can gain a qualitative understanding of the collapse and revival from an analysis of the matrix elements of the operators J^+ and J^-, which give an estimate of the transition frequencies for the atoms from p_i to p_f: although for an initial Fock state the system starts in a state of definite m, it evolves over time into a linear superposition of m states. The matrix elements of J^+ and J^- between different m states yield different Rabi frequencies and hence Bragg oscillation periods. Eigenstates of J^z with eigenvalues m and $m+1$ are coupled by the matrix element

$$\langle j,m+1|J^+|j,m\rangle = \sqrt{(j+m+1)(j-m)}. \quad (13)$$

We can therefore estimate the collapse time T_{decay} by calculating the difference between the fastest and the slowest of these frequencies, the collapse time being roughly the time after which this frequency difference has produced a phase difference of 2π. Under the assumption that all m states contribute equally to the dynamics we find

$$T_{\text{decay}} = \frac{2\pi g^{-1}}{\langle j,1|J^+|j,0\rangle - \langle j,j|J^+|j,j-1\rangle} = \frac{2\pi g^{-1}}{\sqrt{(j+1)j} - \sqrt{2j}}. \quad (14)$$

This estimate gives satisfactory agreement with the actual decay time for small j (it is within $\sim 10\%$ of the numerical result for our parameters), but breaks down for large j. We attribute this to the fact that the assumption that all m states are initially equally populated is unphysical for large j.

The revival time of the Pendellösung oscillations can be evaluated in a similar fashion: The revivals occur when the Rabi frequencies for neighboring m-states differ in phase by 2π. This gives
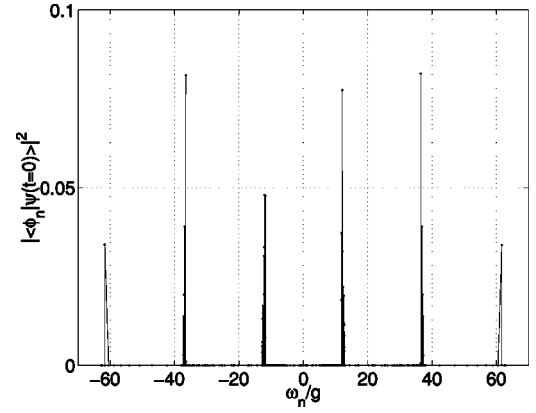

FIG. 8. Projection of the initial conditions onto the spectrum of the Hamiltonian (11) for $N_q=N_{-q}=6$ photons, five atoms, a recoil energy of $E_{2q}=50g$, and a Fermi momentum of $k_F=0.1q$. Eigenfrequencies in units of g.

$$T_{\text{revival}} = \frac{2\pi g^{-1}}{\langle j,1|J^+|j,0\rangle - \langle j,2|J^+|j,1\rangle}$$

$$= \frac{2\pi g^{-1}}{\sqrt{(j+1)j} - \sqrt{(j+2)(j-1)}}, \quad (15)$$

which goes to infinity when $j \to \infty$. Note that this estimate is not limited to small j values since it does not rest on the assumption of equal populations of all m states.

The collapse and revival times can be analyzed more quantitatively from the spectrum of the Hamiltonian. We numerically determined the eigenvectors $|\phi_n\rangle$ and the eigenfrequencies ω_n. Figure 8 shows the projection $|\langle \phi_n|\psi(t=0)\rangle|^2$ of the initial state $|\psi(t=0)\rangle$ onto the numerically determined eigenstates $|\phi_n\rangle$

$$H|\phi\rangle = \omega_n|\phi_n\rangle,$$

of the Hamiltonian as a function of the corresponding eigenfrequencies ω_n. While the eigenfrequencies cover the whole spectrum rather densely, the initial state of the system is well described as a superposition of just a few groups of eigenstates, and hence only a few narrow bands of frequencies, which turn out to be almost equally spaced, significantly determine the atomic dynamics. If these frequency bands were exactly evenly spaced the Pendellösung oscillations would be perfectly periodic. The variations in spacing and widths of the various frequency bands lead to the more complicated dynamics.

The width of the frequency bands, which can be traced back to the usual dephasing of the atoms due to their spread in kinetic energies, gives the ordinary decay of the density oscillations, while the variation in separations between bands is a measure of the inverse revival time. Figure 9 shows this separation, obtained numerically for several photon numbers with and without dephasing. For comparison we also give the inverse revival time as determined from the matrix elements of J^+ as well as by a direct inspection of $N_{sc}(t)$. While the agreement between the revival times determined from the spectrum of the Hamiltonian and from $N_{sc}(t)$ is good for all
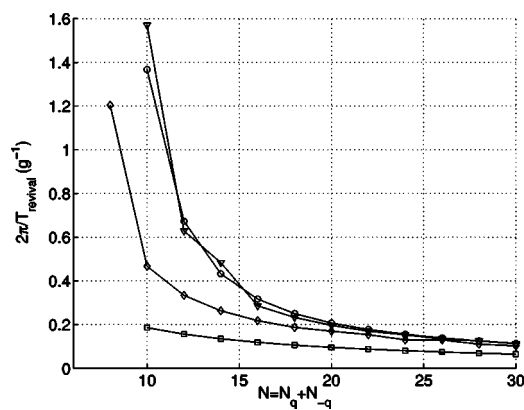
FIG. 9. Inverse revival time $2\pi/T_{\text{revival}}$ of the oscillations as determined from the spectrum of the Hamiltonian as a function of the photon number for $E_{2q}=50g$ and $k_F=0.1q$ ($\diamond$). For comparison we also show the results without dephasing, $k_F=0$ ($\bigcirc$) and the values obtained from comparing matrix elements of J^+, i.e., $\sqrt{(j+1)j}-\sqrt{(J+2)(j-1)}$ ($\square$). The inverse revival times as determined directly from simulations for $N_{sc}(t)$ like the one shown in Fig. 7(b) for no dephasing are also give ($\triangledown$). Frequencies are in units of g.

photon numbers, the agreement with the estimate based on the matrix elements of J^+ improves for large photon numbers.

2. Coherent state

The case of a coherent state is readily obtained by averaging the Fock state results over a Poissonian photon distribution. The results for $P_{p_f}(t)$ and $N_{sc}(t)$ are given in Figs. 10(a) and 11(a), respectively. The oscillations of the mean number of scattered atoms as well as the Pendellösung oscillations of the individual atoms decay in a time $\lesssim g^{-1}$. In addition to the effects discussed in the previous section, we now have an additional dephasing due to the photon statistics of the coherent states. These independent dephasing processes are normally associated with noncommensurate decay rates and revival times; hence there are no revivals in this case.

C. Bloch vector model

We mentioned that since in the Bragg regime the atoms undergo Pendellösung oscillations between two momentum states, they can be thought of as two-level systems, albeit in momentum space rather than in energy. This two-level structure suggests that we recast the problem in the language of Bloch vectors well known from conventional quantum optics. We proceed by introducing the pseudospin vector

$$\mathbf{S_k} = S_k^x \hat{\mathbf{x}} + S_k^y \hat{\mathbf{y}} + S_k^z \hat{\mathbf{z}},$$

where $\hat{\mathbf{x}}$, $\hat{\mathbf{y}}$, and $\hat{\mathbf{z}}$ are unit vectors along the x, y, and z directions in the abstract Bloch vector space and

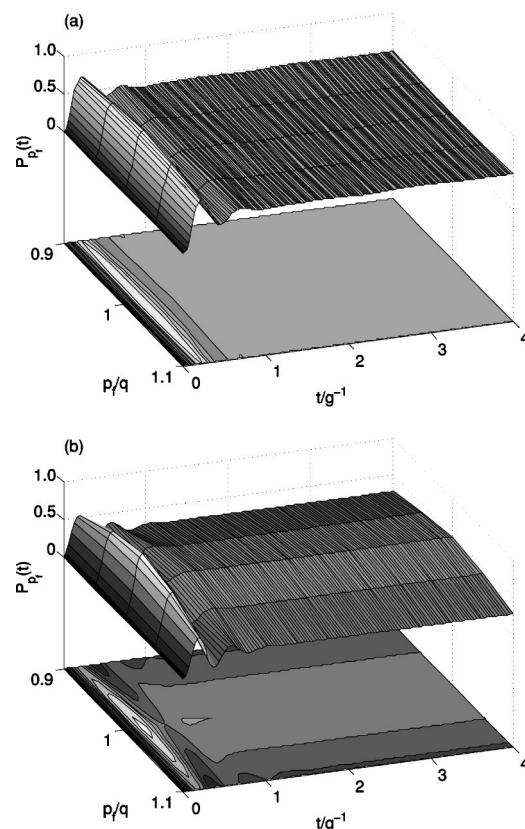$$S_k^x = \frac{1}{2}(S_k^+ + S_k^-),$$

FIG. 10. Scattering probability for five atoms scattering off (a) a running wave and (b) a standing wave in a coherent state. In both cases the recoil energy is $E_{2q}=50g$ and the Fermi momentum is $k_F=0.1q$. The mean number of photons is $\bar{N}_q=\bar{N}_{-q}=6$ in (a) and $\bar{N}=12$ in (b). Time is in units of g^{-1} and momentum in units of q.
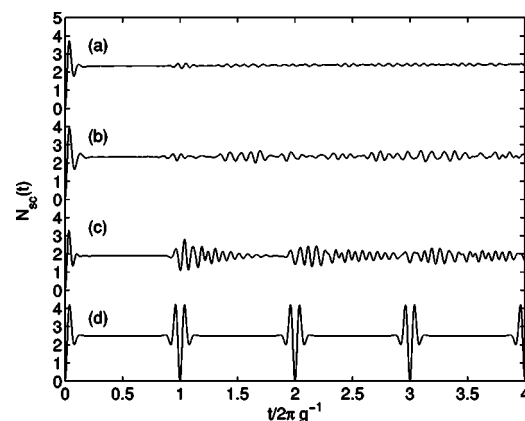

FIG. 11. Mean number of scattered atoms $N_{sc}(t)$ in coherent state light fields. (a) Running-wave light field with mean photon numbers $\bar{N}_q=\bar{N}_{-q}=6$. The Fermi momentum is $k_F=0.1q$ and the recoil energy is $E_{2q}=50g$. (b) Light field as in (a), atoms without dephasing, i.e., $k_F=0$. (c) Standing-wave light field with mean photon number $\bar{N}=12$ and Fermi momentum $k_F=0.1q$ and recoil energy $E_{2q}=50g$. (d) Light field as in (c), but without dephasing for the atoms, $k_F=0$. Time in units of $2\pi g^{-1}$.
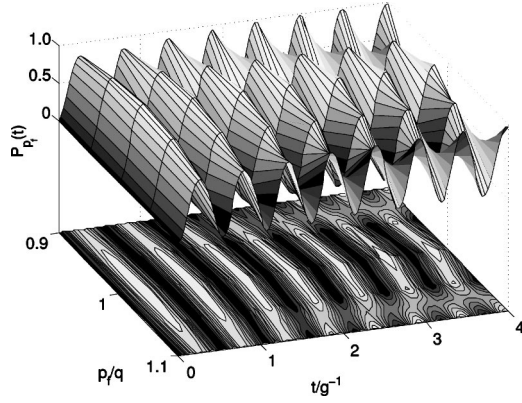
FIG. 12. Scattering probability $P_{p_f}(t)$ for five atoms in a running-wave light field as calculated within the Bloch vector picture. The Fermi momentum is $k_F = 0.1q$ and the recoil energy is $E_{2q} = 50g$. Time in units of g^{-1} and momentum in units of q.

$$S_k^y = \frac{1}{2i}(S_k^+ - S_k^-) \tag{16}$$

[see Eq. (9)]. The operators S_k^l, $l = x, y, z$, obey the usual angular momentum commutation relations

$$[S_k^l, S_{k'}^m] = i\epsilon_{lmn}\delta_{k,k'}S_k^n, \tag{17}$$

where ϵ_{lmn} is the Levi-Cività symbol. Using these commutation relations we obtain the coupled equations of motion for the light field and atomic operators (11):

$$\frac{d\mathbf{J}}{dt} = g(S^x\hat{\mathbf{x}} + S^y\hat{\mathbf{y}}) \times \mathbf{J},$$

$$\frac{d\mathbf{S}_k}{dt} = [\delta\omega_k\hat{\mathbf{z}} + g(J^x\hat{\mathbf{x}} + J^y\hat{\mathbf{y}})] \times \mathbf{S}_k, \tag{18}$$

where we have introduced the total atomic spin operators

$$S^l = \sum_k S_k^l.$$

Equations (18) are exact within the two-state picture of Bragg scattering. We can then obtain a semiclassical version of these equations by factorizing expectation values of products of atomic and field operators, e.g., $\langle S^m J^n \rangle = \langle S^m \rangle \langle J^n \rangle$.

For atoms with initial momenta centered around $-q$ we have $\langle S_k^z(0) \rangle = -1/2$, $\langle S_k^x(0) \rangle = \langle S_k^y(0) \rangle = 0$ for all k, so that the individual atomic Bloch vectors point to the south pole. Likewise, for a field in a Fock state we have that $\langle J^x(0) \rangle = \langle J^y(0) \rangle = 0$, so that $\mathbf{J}$ points along the $\hat{\mathbf{z}}$ axis, too. From the Bloch equations (18) it is then immediately apparent that there is no atomic scattering in the semiclassical description, consistently with the previous discussion.

For a coherent state, on the other hand, $\mathbf{J}$ is not parallel to the z axis. For our choice of phase and for $\bar{N}_q = \bar{N}_{-q}$, it points instead along the x direction. The phase relationship between the two counterpropagating coherent states leads to an intensity grating and the atoms will scatter off it. Figure 12 shows the resulting scattering probability $P_{p_f}(t)$ obtained from this

approximate model for five atoms and a light field initially in a coherent state with mean photon numbers $\bar{N}_q = \bar{N}_{-q} = 6$.

The atomic Pendellösung oscillations do not decay as fast as in the full quantum description of Fig. 10(a). In the present picture, it can be attributed to the degradation of the intensity grating. The maximum oscillation amplitude occurs when $\mathbf{J}$ lies in the equatorial $\hat{\mathbf{x}}$-$\hat{\mathbf{y}}$ plane, but the scattering of the atoms leads to a redistribution of the photons between the counterpropagating modes and a decrease in the optical fringe visibility.

IV. STANDING-WAVE QUANTIZATION

For a standing-wave quantization of the light field the Hamiltonian (2) is replaced by

$$H_s = \sum_k E_k c_k^\dagger c_k + \frac{g\hat{N}}{2}\sum_k c_{k-q}^\dagger c_{k+q} + \text{H.c.} \tag{19}$$

where $\hat{N} = a^\dagger a$, the number operator for the optical field mode, is clearly a constant of motion, and $a^\dagger$ and a are bosonic creation and annihilation operators.

A. Raman-Nath regime

From Eq. (19) we now have

$$i\frac{d}{dt}c_{k_1}^\dagger c_{k_2} = (E_{k_2} - E_{k_1})c_{k_1}^\dagger c_{k_2} + \frac{g\hat{N}}{2}(c_{k_1}^\dagger c_{k_2-2q} + c_{k_1}^\dagger c_{k_2+2q})$$

$$- \frac{g\hat{N}}{2}(c_{k_1+2q}^\dagger c_{k_2} + c_{k_1-2q}^\dagger c_{k_2}). \tag{20}$$

Since Eq. (19) does not couple states with different photon numbers, we can replace $\hat{N}$ by the corresponding eigenvalue N for a particular number state $|N\rangle$. We can then calculate the evolution of $\langle c_{k_1}^\dagger c_{k_2} \rangle$ for a general state of the field by averaging over the appropriate photon number distribution.

The equations for the first-order moments of the individual atoms are identical to those describing the scattering of a single atom by a classical light field, if one identifies $gN/2$ with the classical Rabi frequency. This follows from the absence of correlations between the light field and the atoms, together with the condition $q > k_F$, which implies the absence of Pauli blocking.

The scattering of a single atom by a classical field is a well-studied problem. An analytical solution is known in the Raman-Nath regime; see, e.g., [18,22,23]. If the kinetic energy of the atoms is not negligible, on the other hand, one has to rely on a numerical solution.

Figure 13 shows the results for two atoms in a Fock state with $N = 6$ photons. For short times the scattering clearly resembles the single-particle behavior, the probability of finding an atom in the mth side mode being proportional to $J_m^2(gNt)$. Note that this result is identical to the approximate first-order calculation for the running-wave coherent state of Sec. III.

The solution for a coherent state is obtained by averaging over a Poissonian photon number distribution. The result is
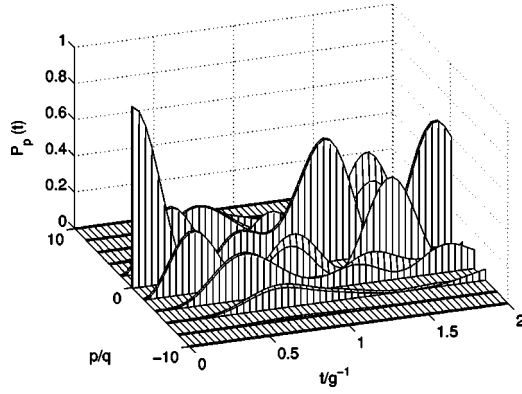
FIG. 13. Scattering of two atoms off a standing-wave light field in a Fock state with $N=6$ photons; the recoil energy is $E_{2q}=g$ and the Fermi momentum is $k_F=0.1q$. Time in units of g^{-1} and momentum in units of photon momentum q.

shown in Fig. 14 for a mean photon number $\bar{N}=6$, which illustrates the dephasing due to the distribution of Rabi frequencies for such a state.

B. Bragg regime

As previously discussed, the atoms can now be described in a two-state basis, leading to the effective Hamiltonian [see Eq. (11)]

$$H = \sum_{k \in [-k_F, k_F]} \left\{ \delta\omega_k S_k^z + \frac{g\hat{N}}{2}(S_k^- + S_k^+) \right\}. \quad (21)$$

Evidently, the Hamiltonian decomposes into independent single-particle Hamiltonians for the individual atoms, $H = \Sigma_k H_k$, so that the atomic equations of motion decouple and can be readily solved analytically. If the cavity is in a Fock state, the atoms undergo Pendellösung oscillations independently of each other, with a detuning given by $\delta\omega_k$. We then obtain
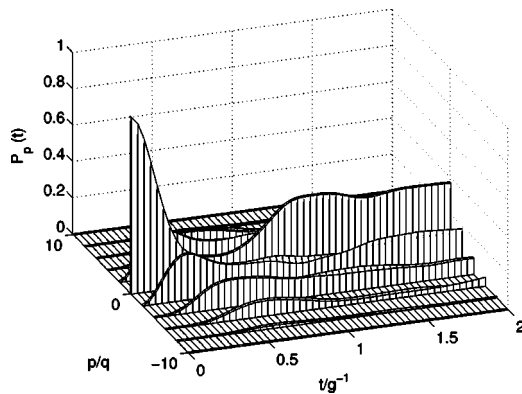

FIG. 14. Scattering of two atoms off a standing-wave light field in a coherent state. The mean number of photons is six, the recoil energy is $E_{2q}=g$, and the Fermi momentum is $k_F=0.1q$. Time in units of g^{-1} and momentum in units of photon momentum q.

$$P_{p_f}(t) = \frac{(gN/2)^2}{\delta\omega_k^2 + (gN/2)^2} \sin^2(\sqrt{\delta\omega_k^2 + (gN/2)^2}\,t), \quad (22)$$

as illustrated in Fig. 6(b) for five atoms and the light field in a Fock state with $N=12$ photons. As expected, the frequency of the Pendellösung oscillations increases and their amplitude decreases with detuning [see Eq. (22)]. In contrast to the running-wave case, these oscillations remain perfectly sinusoidal for all times.

The oscillations in the mean number of scattered atoms $N_{sc}(t)$ are shown in Fig. 7(c) for an atom number of 200. All other parameters are as before [24]. Their decay due to the spread in detunings $\delta\omega_k$ resembles the dephasing of an inhomogeneously broadened ensemble of independent two-level systems, with a dephasing time given by $2\pi/\delta\omega_{k_F}$.

The scattering probability for a coherent state light field is shown in Fig. 10(b) and the mean number of scattered atoms $N_{sc}(t)$ is shown in Fig. 11(c). The atomic parameters are the same as for the Fock state calculations while the light field has been replaced by a coherent state with the mean number of photons $\bar{N}=12$.

As in the running-wave case, the oscillations collapse due to the spread in Rabi frequencies associated with the coherent state. In contrast to that former case, though, they also undergo a revival after the time $T_{\text{revival}}=2\pi g^{-1}$, as follows from the fact that the difference between the Rabi frequencies for N and $N+1$ photons is $g/2$, independently of N. As in the two-photon Jaynes-Cumming model, all number states rephase at the same instant and the revivals are perfect if the dephasing due to the kinetic energy of the atoms can be neglected, as shown in Fig. 11(d). With dephasing included, the revivals are only partial; see Fig. 11(c).

Another difference between the running-wave and standing-wave quantization schemes can be seen in the evolution of the scattering probability for the coherent state. In the case of running waves the probability of finding an atom in the scattered states is about 1/2, independently of their detuning, while in the standing-wave case this probability decreases with increasing detuning. This difference underlines the importance of the correlations between the light field and the atoms. While the atoms move independently in a standing-wave light field, the atoms and the field become an inseparable quantum system in the running-wave case.

V. CONCLUSION AND OUTLOOK

In this paper we have compared the scattering of ultracold fermions by quantized light fields composed of "true" standing waves and of superpositions of counterpropagating running waves, both in the Raman-Nath and in the Bragg regimes. The central difference between the two quantization schemes is that the entanglement between the light field and the atoms plays a crucial role for a running-wave light case, but not for standing-wave quantization.

In the Raman-Nath regime the scattering by a standing-wave light field in a Fock state is similar to the scattering by a classical field, and can be largely understood from the results for a single atom. The only many-particle effect is a dephasing of the atomic motion due to the finite width of the

TABLE I. Time scales for the different processes that lead to a collapse and revival of the Bragg oscillations.

Decay mechanism	Present in				Collapse time	Revival time
	Fock state, standing wave	Fock state, running wave	coherent state, standing wave	coherent state, running wave		
Dephasing due to kinetic energy of atoms	Yes	Yes	Yes	Yes	$2\pi\dfrac{q}{2k_F E_{2q}}$	No revivals
Different Rabi frequencies due to photon number uncertainty	No	No	Yes	Yes	$4\pi/\sqrt{\bar{N}}g$	$2\pi/g$
Correlations between light field and atoms	No	Yes	No	Yes	$\dfrac{4\pi}{g(\sqrt{(N+2)}N - 2\sqrt{N})}$	$\dfrac{4\pi}{g(\sqrt{(N+2)}N - \sqrt{(N+4)(N-2)})}$

initial momentum distribution of the atoms. For running-wave quantization, on the other hand, the quantum correlations that develop between the light field and atoms are essential, and their neglect leads to the absence of atomic diffraction by a Fock state of the field.

In the Bragg regime and for a standing-wave light field, atomic diffraction can be solved in terms of solutions for single atoms, which undergo Pendellösung oscillations that undergo a series of collapse and revivals in the case of a coherent light field. For the case of running-wave quantization, these oscillations decay even for a Fock state, a consequence of the correlations that develop between the light field and the atoms. A coherent state merely leads to a faster collapse.

Table I gives a summary of the mechanisms that lead to collapses and possibly revivals in the various cases that we have discussed, as well as the associated time scales.

This paper has considered only fermionic atoms. Bosonic operators commute rather than anticommute, resulting in different equations of motion for the second and higher correlation functions of atomic operators. Consequently, differences in the scattering result solely from the effect of these higher-order correlations on the dynamics.

[1] M. H. Anderson, J. R. Ensher, M. R. Mathews, C. E. Wieman, and E. E. Cornell, Science **269**, 198 (1995).

[2] C. C. Bradley, C. A. Sackett, J. J. Tollett, and R. G. Hulet, Phys. Rev. Lett. **75**, 1687 (1995).

[3] K. Davis, M. O. Mewes, M. R. Andrews, N. J. van Druten, D. S. Durfee, D. M. Kurn, and W. Ketterle, Phys. Rev. Lett. **75**, 3969 (1995).

[4] C. A. Regal, M. Greiner, and D. S. Jin, Phys. Rev. Lett. **92**, 040403 (2004).

[5] Z. Hadzibabic, S. Gupta, C. A. Stan, C. H. Schunck, M. W. Zwierlein, K. Dieckmann, and W. Ketterle, Phys. Rev. Lett. **91**, 160401 (2003).

[6] K. E. Strecker, G. B. Partridge, and G. Hulet, Phys. Rev. Lett. **91**, 80406 (2003).

[7] F. Burgbacher and J. Audretsch, Phys. Rev. A **60**, 3385 (1999).

[8] S. Inouye, A. P. Chikkatur, D. M. Stamper-Kurn, J. Stenger, and W. Ketterle, Science **285**, 571 (1999).

[9] M. Kozuma, Y. Suzuki, Y. Torii, T. Sigiura, T. Kuga, E. E. Hagley, and L. Deng, Science **286**, 2309 (1999).

[10] S. Inouye, T. Pfau, S. Gupta, A. P. Chikkatur, A. Görlitz, D. E. Pritchard, and W. Ketterle, Nature (London) **402**, 641 (1999).

[11] C. K. Law and N. P. Bigelow, Phys. Rev. A **58**, 4791 (1998).

[12] D. Jaksch, C. Bruder, J. I. Cirac, and P. Zoller, Phys. Rev. Lett. **81**, 3108 (1998).

[13] M. Greiner, O. Mandel, T. Esslinger, T. W. Hänsch, and I. Bloch, Nature (London) **415**, 39 (2002).

[14] M. Greiner, O. Mandel, T. W. Hänsch, and I. Bloch, Nature (London) **419**, 51 (2002).

[15] M. Moore, O. Zobay, and P. Meystre, Phys. Rev. A **60**, 1491 (1999).

[16] G. Lenz, P. Lax, and P. Meystre, Phys. Rev. A **48**, 1707 (1993).

[17] B. Shore, P. Meystre, and S. Stenholm, J. Opt. Soc. Am. B **8**, 903 (1991).

[18] P. Meystre and M. Sargent III, *Elements of Quantum Optics*, 3rd ed. (Springer-Verlag, Berlin, 1999).

[19] K. Huang, *Statistical Mechanics* (John Wiley & Sons, New York, 1987).

[20] J. R. Anglin and A. Vardi, Phys. Rev. A **64**, 013605 (2001).

[21] R. P. Feynman, *Statistical Mechanics* (W. A. Benjamin, Reading, MA, 1972).

[22] A. Rojo, J. Cohen, and P. Berman, Phys. Rev. A **60**, 1482 (1999).

[23] C. P. Search, H. Pu, W. Zhang, and P. Meystre, Phys. Rev. Lett. **88**, 110401 (2002).

[24] This comparatively large number of atoms is to avoid artifical revivals resulting from a finite quantization volume in the numerics, which are the only dephasing effect in the present case. In all other cases the frequency differences between the atoms are smaller than all other frequencies in the systems so that the associated revivals show up only at much later times.